# Strategies for state space restriction in densely coupled spin systems with applications to spin chemistry

H. J. Hogben,[1] P. J. Hore,[1] and Ilya Kuprov[2,a)]
[1]*Department of Chemistry, Physical and Theoretical Chemistry Laboratory, University of Oxford, South Parks Road, Oxford OX1 3QZ, United Kingdom*
[2]*Oxford e-Research Centre, University of Oxford, 7 Keble Road, Oxford OX1 3QG, United Kingdom*

(Received 3 December 2009; accepted 29 March 2010; published online 4 May 2010)

We propose three basis screening methods for state space restriction in Liouville space simulations of large densely coupled spin systems encountered in electron paramagnetic resonance (EPR) spectroscopy and spin chemistry. The methods are based on conservation law analysis, symmetry factorization, and the analysis of state space connectivity graphs. A reduction in matrix dimensions by several orders of magnitude is demonstrated for common EPR and spin chemistry systems. © *2010 American Institute of Physics*. [doi:10.1063/1.3398146]

## I. INTRODUCTION

The last few years have seen growing evidence that in many classes of quantum dynamics processes only a small fraction of the full state space is ever populated. Spin dynamics is no exception, and approaches have recently been developed for efficient simulation of large spin systems using "state space restriction" methods to eliminate redundant states.[1–3] Liquid-state nuclear magnetic resonance (NMR) simulations of systems with hundreds of spins can now be performed routinely[1,2] and there are encouraging signs that something similar will be possible for solid state NMR.[3]

The dimension of the state space of a single particle with spin quantum number $S$ is $(2S+1)^2$, corresponding to the number of independent elements in the spin density matrix. Because the state space of a multispin system is a direct product of single-spin spaces, its dimension, $\Pi_k(2S_k+1)^2$, quickly becomes prohibitively large, necessitating some kind of basis transformation to reduce the size of the matrices required to describe the dynamics. This is often possible,[1,2] and the objective of formally exact state space restriction is to find a minimal basis that spans the system trajectory under a given Hamiltonian.[2,4,5] The system can then be projected into this basis at the start of the simulation and the calculation carried out (not necessarily in the time domain) with reduced matrices. Our previous articles used interaction topology[1] and Krylov subspace analysis[2] to achieve state space reduction. In solid state NMR, nonselective truncation of all spin orders involving more than four spins was recently shown to be successful in predicting the spectra of spinning powders.[3]

In the treatment below we explore specialized algebraic criteria based on conservation laws, symmetries and the connectivity of the Liouville space to demonstrate that after redundant states have been eliminated, the matrix dimensions required for accurate spin dynamics simulations in radicals and radical pairs are, in fact, surprisingly small. It is shown that the superoperators can be constructed directly in the reduced basis, which is a more efficient procedure than pruning the complete state space superoperators.[2,4,5] The proposed state space restriction techniques allow Liouville-space simulation (with all its benefits, such as accurate relaxation and chemical kinetics superoperators) of spin systems of previously prohibitive size.

a)FAX: +44 1865 610612. Electronic mail: ilya.kuprov@oerc.ox.ac.uk.

## II. STATE SPACE REDUCTION STRATEGIES

This section provides a rigorous (and therefore rather involved) foundation for the state space restriction methods proposed in this paper. A reader looking for practical examples may wish to skip to Sec. IV and/or download the latest version of the SPINACH library (http://spindynamics.org) which includes a MATLAB implementation of these tools.

### A. Conservation law pruning

One of the simplest analytical methods for state space reduction is to eliminate all states that violate conservation laws. If the observable corresponding to an operator $\hat{A}$ is conserved, that is

$$\langle\hat{A}\rangle = \text{const} \Leftrightarrow [\hat{H},\hat{A}] = 0 \Leftrightarrow \hat{\hat{H}}\hat{A} = 0, \tag{1}$$

where $\hat{H}$ and $\hat{\hat{H}}$ are the Hamiltonian operator and superoperator, respectively, then the state subspaces spanned by the eigenstates with the expectation value $\langle\hat{A}\rangle$ that does not match that of the initial state of the system can be weeded out. The actual active subspace is then the intersection of $\langle\hat{A}\rangle$=const subspaces for every linearly independent operator $\hat{A}$ in the null space of $\hat{\hat{H}}$. The states outside that subspace would not be populated and can be discarded.

Furthermore, if the initial density matrix $\hat{\rho}(0)$ is an eigenstate of the commutation superoperator corresponding to $\hat{A}$,

 

$$\hat{\hat{A}}\hat{\rho}(0) = [\hat{A}, \hat{\rho}(0)] = a\hat{\rho}(0), \tag{2}$$

then the corresponding eigenvalue $a$ is also a conserved property, because

$$\hat{\hat{A}}\hat{\rho}(t) = [\hat{A}, e^{-i\hat{H}t}\hat{\rho}(0)e^{i\hat{H}t}] = e^{-i\hat{H}t}[\hat{A}, \hat{\rho}(0)]e^{i\hat{H}t} = a\hat{\rho}(t). \tag{3}$$

The simulation trajectory would therefore be confined to the subspace for which $\hat{\hat{A}}\hat{\rho}(t) = a\hat{\rho}(t)$. Because Eqs. (2) and (3) are linear with respect to $\hat{\rho}(t)$, the subspaces with different values of $a$ would not interact and may be simulated separately if the system starts off in a linear combination of eigenoperators of $\hat{\hat{A}}$.

Equation (1) shows that the number of such observables is equal to the dimension of the null space of $\hat{\hat{H}}$, which is equal to the number of small eigenvalues in $\hat{\hat{H}}$ (the term *small* in this context is understood as small enough to be inconsequential on the time scale of the simulation). The resulting conservation laws need not be easily interpretable, but the simple quantities often conserved during evolution of common spin systems are the total spin $\hat{S}^2$ and the total $Z$-component of spin $\hat{S}_Z$:

$$\hat{S}^2 = \sum_{n,k}\left(\hat{S}_Z^{(n)}\hat{S}_Z^{(k)} + \tfrac{1}{2}(\hat{S}_+^{(n)}\hat{S}_-^{(k)} + \hat{S}_-^{(n)}\hat{S}_+^{(k)})\right);$$
$$\hat{S}_Z = \sum_k \hat{S}_Z^{(k)}. \tag{4}$$

If the basis set is chosen to be the eigenstates of $\hat{\hat{A}}$ (e.g., direct products of irreducible spherical tensors $\hat{T}_{lm}$ in the case of $\hat{\hat{S}}^2$ and $\hat{\hat{S}}_Z$) a fast basis screening procedure can be implemented, leading to a significant (see the examples in Sec. IV) reduction in problem dimensionality.

### B. Symmetry pruning

In symmetric spin systems (e.g., those with magnetically equivalent nuclei),[6–8] the operators from the symmetry group commute with the Hamiltonian, meaning that the subspaces that are invariant under the symmetry group are also invariant under the Hamiltonian. The group-theoretical procedure for generating the symmetry-adapted basis set is well known[8–10] and results in block diagonalization of the Hamiltonian with the associated computational benefits (individual blocks may be simulated separately). In Liouville space, however, the situation acquires an interesting twist—we will now demonstrate that in many practical cases the only irreducible representation (irrep) that needs to be simulated in Liouville-space is $A_{1g}$, otherwise known as $\Sigma_g^+$, or the "fully symmetric" irreducible representation.

This difference in symmetry behavior of Hilbert and Liouville spaces may be illustrated on a two-spin system; while the singlet state wavefunction does change sign under spin permutation in Hilbert space,

$$\hat{P}_{12}(|\alpha\beta\rangle - |\beta\alpha\rangle) = |\beta\alpha\rangle - |\alpha\beta\rangle = -(|\alpha\beta\rangle - |\beta\alpha\rangle), \tag{5}$$

its representation in Liouville space does not:

$$\hat{P}_{12}(|\alpha\beta\rangle - |\beta\alpha\rangle)(\langle\alpha\beta| - \langle\beta\alpha|)\hat{P}_{12}^{\dagger} = (|\alpha\beta\rangle - |\beta\alpha\rangle)(\langle\alpha\beta| - \langle\beta\alpha|). \tag{6}$$

More generally, any symmetry-adapted Hilbert space wavefunction belonging to an irrep other than the fully symmetric one,

$$\hat{P}|\psi\rangle = e^{i\varphi}|\psi\rangle, \quad \varphi \in \mathbb{R}, \tag{7}$$

is going to have a fully symmetric representation in Liouville space because

$$\hat{P}|\psi\rangle\langle\psi|\hat{P}^{\dagger} = e^{i\varphi}|\psi\rangle\langle\psi|e^{-i\varphi} = |\psi\rangle\langle\psi|. \tag{8}$$

It does therefore appear that irreducible representations other than $A_{1g}$ get "symmetrized" into $A_{1g}$ during the Hilbert to Liouville space transformation.

It also appears that the system evolution in Liouville space stays confined to $A_{1g}$ — in the most general case, it is governed by the following equation:

$$\frac{\partial\hat{\rho}}{\partial t} = -\mathrm{i}\hat{\hat{H}}\hat{\rho} + \hat{\hat{K}}\hat{\rho} + \hat{\hat{R}}(\hat{\rho} - \hat{\rho}_{\mathrm{eq}}), \tag{9}$$

where $\hat{\rho}$ is the density matrix, $\hat{\rho}_{\mathrm{eq}}$ is the equilibrium density matrix, $\hat{\hat{H}}$ is the Hamiltonian commutation superoperator, $\hat{\hat{K}}$ is the chemical kinetics and spatial diffusion superoperator, and $\hat{\hat{R}}$ is the relaxation superoperator obtained using one of the available relaxation theories.[11–16] The Hamiltonian commutation superoperator $\hat{\hat{H}} = [\hat{H}, \cdot] = \hat{H}\otimes\hat{E} - \hat{E}\otimes\hat{H}^{\mathrm{T}}$, where $\hat{E}$ is the identity operator, inherits the symmetry of the Hamiltonian which commutes with the symmetry group, meaning that $\hat{\hat{H}} \in A_{1g}$. If the user declared some spins "equivalent" in a system undergoing chemical reactions, they must be transported as such in any chemical process, meaning that, by definition, $\hat{\hat{K}} \in A_{1g}$. The initial state of the system is either thermodynamic equilibrium, which inherits the $A_{1g}$ symmetry of the Hamiltonian via

$$\hat{\rho}_{\mathrm{eq}} = \frac{\exp[-\hat{H}/k_{\mathrm{B}}T]}{\mathrm{Tr}(\exp[-\hat{H}/k_{\mathrm{B}}T])}, \tag{10}$$

or a user-supplied nonequilibrium state, which is fully symmetric by definition with respect to the spins that the user declared equivalent. The case of the relaxation superoperator is somewhat more involved, given that many theories of relaxation exist in the literature. In the most popular case of the Redfield superoperator[15,16]

$$\hat{\hat{R}}(\hat{\rho} - \hat{\rho}_{\mathrm{eq}}) = \int_0^{\infty} \overline{[\hat{H}_1(0), [\mathrm{e}^{i\hat{H}_0\tau}\hat{H}_1(\tau)\mathrm{e}^{-i\hat{H}_0\tau}, \hat{\rho} - \hat{\rho}_{\mathrm{eq}}]]}\,\mathrm{d}\tau. \tag{11}$$

Under the assumption that the stochastic part $\hat{H}_1(t)$ of the Hamiltonian obeys the system symmetry, the entire double commutation superoperator on the right hand side inherits the symmetry of $\hat{H}_0$ and $\hat{H}_1(t)$, which is $A_{1g}$. Noting that the direct product of any number of fully symmetric irreps is itself a fully symmetric irrep completes the proof.

This is a very remarkable fact — it appears that the spin system cannot break out of the fully symmetric irrep because all events and operators affecting it belong to $A_{1g}$. The user can of course push the system out of $A_{1g}$ by deliberately breaking the assumptions we made above, but it would not happen spontaneously. For our purposes, this means that, in Liouville space, any symmetry adapted linear combinations (SALCs) of basis vectors not belonging to the fully symmetric irrep of the system symmetry group can be pruned out. In those rare situations where the assumptions made above do get broken, keeping all irreducible representations still carries a computational benefit, because the Liouvillian is block-diagonal in the symmetry-adapted basis.

Having established the basic properties above, we will now proceed to build the symmetry-adapted basis. The procedure for generating the SALCs is well known[9,10,17,18] and involves line-by-line multiplication of the group action table by the character table to produce the symmetry-adapted operator basis $\{\hat{O}_k^{(\Gamma)}\}$ from the initial product operator basis $\{\hat{O}_k\}$:

$$\hat{O}_k^{(\Gamma)} = \frac{1}{N}\sum_{g\in G} \chi_g^{(\Gamma)} g(\hat{O}_k), \tag{12}$$

where $N$ is the normalization constant, the summation is carried over the individual elements $g$ of the symmetry group $G$, $\chi_g^{(\Gamma)}$ is the character of irreducible representation $\Gamma$ of the group element $g$, and $g(\hat{O}_k)$ is the result of the action by that group element on the basis operator $\hat{O}_k$. The group action $g:\{\hat{O}_k\}\rightarrow\{\hat{O}_k\}$ is an automorphism of the system state space that amounts to permutation of the order of the direct product components of $\{\hat{O}_k\}$.

If multiple groups of equivalent spins described by different symmetry groups are present, the total system symmetry group is a product of the individual groups and the total character table is therefore the direct product of character tables of the individual groups.[17] For a pair of irreducible representations $\Gamma$ and $\Lambda$ of groups $G$ and $H$, respectively,

$$G\times H = \{gh | g\in G, h\in H\} \quad \chi_{gh}^{(\Gamma\times\Lambda)} = \chi_g^{(\Gamma)}\chi_h^{(\Lambda)}. \tag{13}$$

While Hilbert space formulation would have to make use of Eqs. (12) and (13) in their general form, significant simplification is achieved in Liouville space by making use of the above noted fact that only the fully symmetric irrep is ever necessary. Specifically, all characters of $\Gamma = A_{1g}$ of any group are equal to 1, and Eq. (12) is simplified into

$$\hat{O}_k^{(A_{1g})} = \frac{1}{N}\sum_{g\in G} g(\hat{O}_k), \tag{14}$$

that is, the basis simply needs to be fully symmetrized with respect to all operations contained in the total system symmetry group. This means that in a given set of symmetry-related basis operators,

$$\{\hat{O}, g_1(\hat{O}), \ldots, g_{|G|}(\hat{O}) | g_k \in G\},$$

only the fully symmetric linear combination survives and all else is discarded. For example, in a simple case of $S_2$ symmetry group relating two spins in a larger spin system in a Cartesian product operator basis:

$$\begin{cases} \cdots\otimes\hat{L}_Z\otimes\hat{S}_Y\otimes\cdots \\ \cdots\otimes\hat{S}_Y\otimes\hat{L}_Z\otimes\cdots \end{cases}$$
$$\Downarrow$$
$$\begin{cases} \cdots\otimes(\hat{L}_Z\otimes\hat{S}_Y+\hat{S}_Y\otimes\hat{L}_Z)\otimes\cdots & \text{(retained)} \\ \cdots\otimes(\hat{L}_Z\otimes\hat{S}_Y-\hat{S}_Y\otimes\hat{L}_Z)\otimes\cdots & \text{(discarded)}. \end{cases} \tag{15}$$

The resulting basis dimension reduction factor is equal to the order of the full system symmetry group. In common NMR and EPR systems this factor often exceeds 100, meaning a "free" calculation speed-up by a factor of over $10^6$, given the cubic scaling of many matrix operations. Some examples are given in Sec. IV.

It should be noted that, unlike the better known Clebsch–Gordan procedure,[19] the SALC algorithm is agnostic to the spin quantum number; Eqs. (12) and (13) make no reference to the nature of the direct product basis $\{\hat{O}_k\}$, which may contain spin operators of any rank. The symmetrization function currently implemented in the SPINACH library takes full advantage of Eq. (13) and can handle multiple groups of symmetry-related spins of any quantum number.

### C. Separation of noninteracting subspaces

Even in densely coupled spin systems, the Liouvillian superoperator is normally very sparse, meaning that a given state is directly connected to a relatively small number of other states. The consequence is that, even in densely coupled spin systems, the state space connectivity network is sparse and may be analyzed efficiently using graph-theoretical techniques. Specifically, the states in the basis may be treated as nodes of a graph, and the off-diagonal elements of the Liouvillian as edges connecting these nodes. In this picture, the Liouvillian becomes the adjacency matrix[20] of the magnetization flow graph, with the infinitesimal propagation step (illustrated schematically in Fig. 1) driving the state populations through the connections existing in that graph.

The disjoint subgraphs (those that are not connected in any way to each other) of the magnetization flow graph correspond to noninteracting subspaces within the spin system. The number of disjoint subgraphs is a topological invariant of the graph[20] and does not depend on the relative amplitude of individual interactions within the spin system. Linearly scaling algorithms[21,22] exist for partitioning sparse graphs into disjoint subgraphs, the most popular ones being the breadth-first and the depth-first search algorithms.[23] Both are well researched, with standard libraries available in MATLAB. In practice, replacing the Liouvillian with a binary matrix

$$P_{nk} = \begin{cases} 1 & \text{if } |\hat{\hat{L}}_{nk}| > \varepsilon \\ 0 & \text{otherwise} \end{cases}, \tag{16}$$

where $\varepsilon$ is a user-supplied tolerance, yields a sparse matrix $\hat{\hat{P}}$ that may be fed directly into Tarjan's graph partitioning

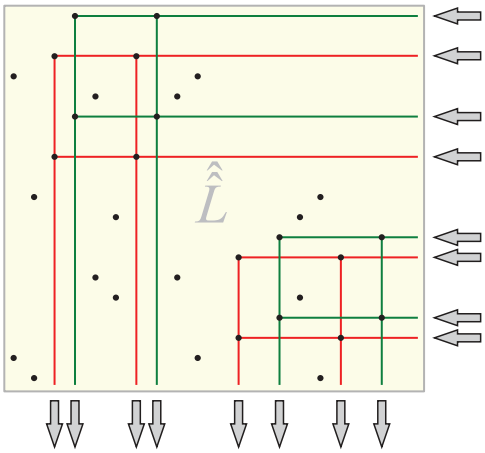

FIG. 1. Schematic of the Liouville space connectivity analysis. The Liouvillian matrix (which is very sparse even in densely coupled spin systems because the Hamiltonian only contains one- and two-spin operators) may be treated as the adjacency matrix of the state space connectivity graph. The dots denote nonzero elements in the Liouvillian and the lines show the coherence transfer paths in an infinitesimal propagation step $\hat{\rho}\rightarrow -i\hat{\hat{L}}\hat{\rho}$. Efficient procedures exist for partitioning sparse graphs into connected subgraphs, which correspond to noninteracting subspaces.

algorithm,[21,22] which returns node lists for the disjoint components of the graph. For our purposes, these are the lists of states populating each of the noninteracting subspaces.

It should be noted that a diagonalization would, of course, achieve the same result — eigenvectors do not interact — but we assume that the system is so large as to render diagonalization (with its cubic scaling in time and memory) unfeasible. Because many ways exist to block diagonalize a given Liouvillian, the improvement resulting from the graph-theoretical analysis does depend on the choice of the basis set. The zero tolerance $\varepsilon$ would normally be set to the minimal interaction amplitude that is deemed significant on the time scale of the simulation, in practice around $10^{-3}t_{\mathrm{sim}}^{-1}$, where $t_{\mathrm{sim}}$ is the simulation trajectory duration, subspaces with cross terms smaller than $\varepsilon$ are deemed disjoint. The simulations in Sec. IV use exact subspace separation with $\varepsilon$ set to zero.

In conclusion to Sec. II, we would observe that the three state space reduction and partitioning methods listed above may be applied sequentially in any order. Even though in practice they tend to produce large independent reductions in the state space (Sec. IV), there is a significant conceptual overlap between the three: symmetry operators commute with the Hamiltonian and may be viewed as conservation laws, and invariant subspaces of the conserved operators are disjoint in the graph-theoretical sense.

## III. SUPEROPERATORS IN THE REDUCED STATE SPACE

In restricted state spaces the standard direct product procedure for operator construction is no longer efficient — producing the full superoperator matrix and then cutting it down would not circumvent the memory problems associated with the storage of the initial large matrices. It is advantageous, therefore, to produce the superoperators directly in the reduced state space.

### A. Basis set indexing

Many complete basis sets have been proposed to suit different objectives in spin dynamics simulations.[24] The most versatile and algebraically appropriate basis set in our experience is direct products of single-spin irreducible spherical tensor operators.[25] One of the key advantages that this basis offers is memory-efficient description of individual states — the indices of the direct product operands uniquely determine the resulting density matrix

$$\hat{T}_{l_1m_1}\otimes\hat{T}_{l_2m_2}\otimes\cdots\otimes\hat{T}_{l_nm_n}\Leftrightarrow\begin{pmatrix} l_1 & l_2 & \cdots & l_n \\ m_1 & m_2 & \cdots & m_n \end{pmatrix}, \tag{17}$$

with memory requirements of $2n$ integer numbers ($n$ is the number of spins) per basis element as opposed to at least $O(2^n)$ double-precision floating-point numbers if the actual density matrix was to be stored. The storage requirements can further be reduced to $n$ integers per basis element if the indexing is linearized, that is, the irreducible spherical tensors are listed by ascending rank, $l$, and within ranks by descending projection quantum number, $m$, and then assigned a number from 0 to $n-1$, beginning with $\hat{T}_{0,0}\equiv$ '0'. The basis set description, once the basis is chosen, is static and any time dependence in the operators or the spin system would only affect their matrix representations in that basis.

### B. Basis set construction

With the indexing convention given by Eq. (17), the basis set description is an array of integers with the number of columns equal to the number of spins in the system and the number of rows equal to the number of states (linearized indexing) or twice the number of states (explicit $l,m$ indexing) in the basis set. The initial basis set can either be complete (only feasible for ten spins or fewer), or uniformly restricted to exclude product states of more than $k<N$ spins,[1,3] or adaptively restricted, with the truncation level depending on the local coupling density.[1] The latter is generally preferred, particularly for large NMR systems; if a spin is coupled to $m$ neighbors, locally including product states of up to $m$ spins appears to be sufficient for most simulation purposes.

After the initial basis is formed and its description stored as prescribed by Eq. (17), the conservation law screening (Sec. II) may be performed using just the indices stored — for example, the eigenvalue of $\hat{\hat{S}}_Z$ (also known as "coherence order") in systems where it is conserved [Eq. (4)] is a simple sum over the $m$ index in Eq. (17):

$$p=\sum_k m_k. \tag{18}$$

Note the complete lack of any matrix operations — we use the general properties of direct products of irreducible spherical tensors without any reference to specific matrix representations.

Similarly, the application of the group action during the SALC procedure in Eq. (12) simply permutes the columns in Eq. (17), effectively exchanging the spins as each symmetry

group element $g$ prescribes. Just as above, the operation is carried out at the basis description level, avoiding the use of explicit operator matrices.

### C. Superoperator construction

After the basis has been pruned, we proceed to generate the superoperators directly in the resulting subspace of the full Liouville space. The basic "building block" superoperators in Liouville space are the left and right product superoperators[24] defined as

$$\hat{\hat{Q}}_{\mathrm{L}}\hat{\rho} = \hat{Q}\hat{\rho}; \quad \hat{\hat{Q}}_{\mathrm{R}}\hat{\rho} = \hat{\rho}\hat{Q}, \tag{19}$$

which perform left and right hand sided multiplication, respectively, by a predefined Hilbert-space operator $\hat{Q}$. The commutation superoperator is then simply the difference between the left and right product superoperators,

$$\hat{\hat{Q}}\hat{\rho} = [\hat{Q},\hat{\rho}] = \hat{Q}\hat{\rho} - \hat{\rho}\hat{Q}, \quad \hat{\hat{Q}} = \hat{\hat{Q}}_{\mathrm{L}} - \hat{\hat{Q}}_{\mathrm{R}}. \tag{20}$$

It would therefore suffice to find an efficient way to generate $\hat{\hat{Q}}_{\mathrm{L}}$ and $\hat{\hat{Q}}_{\mathrm{R}}$ in the reduced basis set. We start by expanding the density operator $\hat{\rho}$ and the generating operator $\hat{Q}$ as linear combinations of the basis operators:

$$\hat{\rho} = \sum_k r_k \hat{O}_k, \quad \hat{Q} = \sum_n q_n \hat{O}_n, \tag{21}$$

where the basis $\{\hat{O}_k\}$ is chosen and indexed according to Eq. (17). The outputs of the right and left multiplication superoperators are then expressed via products of basis operators:

$$\hat{\hat{Q}}_{\mathrm{R}}\hat{\rho} = \sum_{nk} r_k q_n \hat{O}_k \hat{O}_n, \quad \hat{\hat{Q}}_{\mathrm{L}}\hat{\rho} = \sum_{nk} r_k q_n \hat{O}_n \hat{O}_k. \tag{22}$$

Since the spin operators are an algebra, the result of bilinear multiplication is completely determined by the structure coefficients $c_{ijk}$,

$$\hat{O}_i\hat{O}_j = \sum_k c_{ijk}\hat{O}_k, \quad c_{ijk} = \mathrm{Tr}(\hat{O}_i\hat{O}_j\hat{O}_k^{\dagger}), \tag{23}$$

which can be computed (and even precomputed, as happens in SPINACH) extremely efficiently, because they are related in a simple way to the structure coefficients of the operator algebra of a single spin:

$$\begin{aligned} c_{ijk} &= \mathrm{Tr}(\hat{O}_i\hat{O}_j\hat{O}_k^{\dagger}) \\ &= \mathrm{Tr}[(\bigotimes_{n=1}^{N}\hat{T}_{l_{in}m_{in}})(\bigotimes_{n=1}^{N}\hat{T}_{l_{jn}m_{jn}})(\bigotimes_{n=1}^{N}\hat{T}_{l_{kn}m_{kn}})^{\dagger}] \\ &= \mathrm{Tr}[\bigotimes_{n=1}^{N}(\hat{T}_{l_{in}m_{in}}\hat{T}_{l_{jn}m_{jn}}\hat{T}^{\dagger}_{l_{kn}m_{kn}})] \\ &= \prod_{n=1}^{N}\mathrm{Tr}(\hat{T}_{l_{in}m_{in}}\hat{T}_{l_{jn}m_{jn}}\hat{T}^{\dagger}_{l_{kn}m_{kn}}) = \prod_{n=1}^{N} f_{ijk}^{(n)}, \end{aligned} \tag{24}$$

where $f_{ijk}^{(n)}$ are the structure coefficients of the operator algebra of the $n$th spin, written in the irreducible spherical tensor basis, Eqs. (24) and (20), in effect, relate the structure constants of $\mathfrak{su}(2^n)$ to the structure constants of the individual $\mathfrak{su}(2)$ components of the direct product algebra. Given the structure coefficients $c_{ijk}$, the representation of the right and left multiplication superoperators in the $\{\hat{O}_k\}$ basis may be computed efficiently and is given by

$$\begin{aligned} &\hat{\hat{Q}}_{\mathrm{R}}\hat{\rho} = \sum_{nk} r_k q_n \hat{O}_k\hat{O}_n = \sum_{nkm} r_k q_n c_{knm}\hat{O}_m, \\ &[\hat{\hat{Q}}_{\mathrm{R}}\hat{\rho}]_m = \sum_{nk} r_k q_n c_{knm} \Rightarrow [\hat{\hat{Q}}_{\mathrm{R}}]_{mk} = \sum_n q_n c_{knm}, \end{aligned} \tag{25}$$

and similarly for the left hand product superoperator. The simplicity of Eq. (25) and the fact that the structure constants of a single-spin operator algebra can be precomputed (and do not, in fact, even depend on the spin quantum number) mean that the generation of superoperator representations in the restricted state space is a very fast procedure, typically taking seconds even in $10^5$-dimensional state spaces. In practice, a computer stores the small $f_{ijk}^{(n)}$ tables and generates $c_{ijk}$ as necessary from Eq. (24) using $\{\hat{O}_k\}$ descriptions given by Eq. (17). The resulting structure constants and expansion coefficients $q_n$ of the operator $\hat{Q}$ are used in Eq. (25) to calculate the explicit matrix representations of $\hat{\hat{Q}}_{\mathrm{L}}$ and $\hat{\hat{Q}}_{\mathrm{R}}$ in the reduced basis. Once the representations of user-specified superoperators in the reduced basis are available, any conceivable simulation can be performed, the only difference from the standard procedures being the smaller matrix dimensions.

An important property of Eqs. (21)–(25) is favorable scaling with respect to the number of spins $n$ in physically relevant finite-time simulations: if the generating operator $\hat{Q}$ in Eq. (21) is the Hamiltonian, then its expansion has $O(n^2)$ terms (physical systems only have binary couplings). Each structure coefficient $c_{ijk}$ in Eq. (24) requires $O(n)$ multiplications [$\mathfrak{su}(2)$ structure constants $f_{ijk}^{(n)}$ are known and tabulated]. Therefore, the cost of obtaining a matrix representation of the Hamiltonian commutation superoperator using Eq. (25) is $O(n^3k^2)$ multiplications, where $k$ is the size of the basis set. It is known that in systems with sparse connectivity,[26] powder averaging[3] or short trajectory duration,[27] the number of active states in the basis set scales polynomially with the number of spins, meaning that the overall complexity scaling for many practically encountered spin systems is also polynomial.

## IV. APPLICATIONS TO SPIN CHEMISTRY

The methods listed above are given in their most general (and therefore necessarily rather obscure) formulation. Practical examples of application of these tools to real-world spin systems are given below. Since the efficiency of state space restriction algorithms has already been demonstrated in liquid[1,2] and solid[3,27] state NMR, we choose to concentrate here on another area of spin dynamics in which simulation plays an important role: spin chemistry, which deals with the effects of electron and nuclear spin on the rates and yields of chemical reactions of paramagnetic molecules. Spin chemical systems often involve relaxation and chemical kinetics and therefore require simulations in Liouville space.[28–31]

### A. Model system

We shall focus explicitly on the effect of static magnetic fields on the reactions of spin-correlated radical pairs in solution. The spin Hamiltonian of a pair of exchange-coupled radicals A and B is $\hat{H}=\hat{H}_{\mathrm{A}}+\hat{H}_{\mathrm{B}}+\hat{H}_{\mathrm{ex}}$, where

$$\hat{H}_{\mathrm{A}}=\omega_{\mathrm{A}}\hat{S}_Z^{(\mathrm{A})}+\sum_k a_k\left(\hat{S}_Z^{(\mathrm{A})}\hat{S}_Z^{(k)}+\tfrac{1}{2}(\hat{S}_+^{(\mathrm{A})}\hat{S}_-^{(k)}+\hat{S}_-^{(\mathrm{A})}\hat{S}_+^{(k)})\right),$$

$$\hat{H}_{\mathrm{B}}=\omega_{\mathrm{B}}\hat{S}_Z^{(\mathrm{B})}+\sum_m a_m\left(\hat{S}_Z^{(\mathrm{B})}\hat{S}_Z^{(m)}+\tfrac{1}{2}(\hat{S}_+^{(\mathrm{B})}\hat{S}_-^{(m)}+\hat{S}_-^{(\mathrm{B})}\hat{S}_+^{(m)})\right), \tag{26}$$

$$\hat{H}_{\mathrm{ex}}=-2J_{\mathrm{AB}}\left(\hat{S}_Z^{(\mathrm{A})}\hat{S}_Z^{(\mathrm{B})}+\tfrac{1}{2}(\hat{S}_+^{(\mathrm{A})}\hat{S}_-^{(\mathrm{B})}+\hat{S}_-^{(\mathrm{A})}\hat{S}_+^{(\mathrm{B})})\right).$$

The first terms in $\hat{H}_{\mathrm{A}}$ and $\hat{H}_{\mathrm{B}}$ are the electron Zeeman interactions with Larmor frequencies $\omega_{\mathrm{A,B}}$ that depend on the $g$-values of the radicals and the magnetic induction (taken to be along the $Z$ axis). The terms under the sums ($k$ and $m$ labels index the nuclear spins in the two radicals) are the isotropic electron-nuclear hyperfine couplings written in terms of raising and lowering operators, $\hat{S}_{\pm}=\hat{S}_X\pm\mathrm{i}\hat{S}_Y$. The last part of $\hat{H}$ is the two-electron exchange interaction. As is customary in fast-motion liquid state treatments, interaction anisotropies are assumed to be averaged on the time scale of the dynamics in question and are treated using Redfield relaxation theory in the extreme narrowing limit.[15,16]

The evolution of the density operator in the presence of relaxation and chemical processes is given by Eq. (9). The initial state of the radical pair $\hat{\rho}(0)$ is either a pure electronic singlet $\hat{Q}_{\mathrm{S}}$ or triplet $\hat{Q}_{\mathrm{T}}$, depending on the spin state of the chemical precursor:

$$\hat{Q}_{\mathrm{S}}=\tfrac{1}{4}\hat{E}-\hat{S}_Z^{(\mathrm{A})}\hat{S}_Z^{(\mathrm{B})}-\tfrac{1}{2}\hat{S}_+^{(\mathrm{A})}\hat{S}_-^{(\mathrm{B})}-\tfrac{1}{2}\hat{S}_-^{(\mathrm{A})}\hat{S}_+^{(\mathrm{B})},$$

$$\hat{Q}_{\mathrm{T}}=\tfrac{3}{4}\hat{E}+\hat{S}_Z^{(\mathrm{A})}\hat{S}_Z^{(\mathrm{B})}+\tfrac{1}{2}\hat{S}_+^{(\mathrm{A})}\hat{S}_-^{(\mathrm{B})}+\tfrac{1}{2}\hat{S}_-^{(\mathrm{A})}\hat{S}_+^{(\mathrm{B})}. \tag{27}$$

The goal is to simulate the magnetic field dependence of the yield of the reaction products formed selectively from the singlet state of the radical pair. This can be done in a variety of ways, the simplest being for the case when the $\hat{Q}_{\mathrm{S}}$ and $\hat{Q}_{\mathrm{T}}$ states disappear with equal first-order rate constants, $k$ (the "exponential model").[32–34] Then, the ultimate yield of the product formed from the S state is[32]

$$\Phi_{\mathrm{S}}=\frac{k}{M}\int_0^{\infty}\mathrm{Tr}[\hat{Q}_{\mathrm{S}}\hat{\rho}(t)]\mathrm{e}^{-kt}\mathrm{d}t;$$

$$\hat{\rho}(t)=\exp[-\mathrm{i}(\hat{\hat{H}}+\mathrm{i}\hat{\hat{R}})t]\hat{\rho}(0), \tag{28}$$

where $M$ is the total number of nuclear spin configurations in the system (a normalization coefficient). After taking the integral in Eq. (28), one obtains

$$\Phi_{\mathrm{S}}=\frac{k}{M}\mathrm{Tr}[\hat{Q}_{\mathrm{S}}(\mathrm{i}\hat{\hat{H}}-\hat{\hat{R}}+k\hat{\hat{E}})^{-1}\hat{\rho}(0)]. \tag{29}$$

Unless the state space is truncated in some way, calculation of $\Phi_{\mathrm{S}}$ and its field dependence would entail manipulation of enormous matrices with all the attendant computational challenges. For example, a radical pair containing eight protons with non-negligible hyperfine couplings has a Liouville state space of dimension of $\sim 10^6$. However, as Sec. III demonstrates, it is possible to reduce the dimension of the problem.

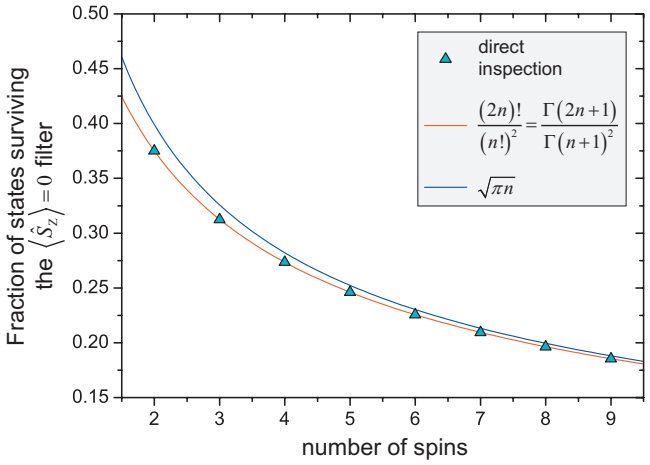


FIG. 2. Fraction of states surviving the $\langle\hat{S}_Z\rangle=0$ conservation filter (and therefore contributing to the spin system evolution) as a function of the total number of spin-1/2 particles in the system.

### B. Conservation law screening

One of the simple observables mentioned in Sec. III, namely, $\langle\hat{S}_Z\rangle$, is conserved under the Hamiltonian in Eq. (26). Because the system starts off in a specific eigenstate of $\hat{\hat{S}}_Z$ for which $[\hat{S}_Z,\hat{Q}_{\mathrm{S}}]=[\hat{S}_Z,\hat{Q}_{\mathrm{T}}]=0$, it will, according to Eq. (3), stay in the $p=0$ subspace indefinitely, and any basis operator with $p=\Sigma_k m_k\neq 0$ [Eq. (18)] would never be populated and may be discarded. In NMR terms, this amounts to restricting the simulation to the zero-quantum subspace, that is to the states with coherence order $p=0$. In a system with $n$ spin-1/2 particles this leads to a reduction in the state space dimension from $4^n$ to $(2n)!/(n!)^2$. Using Stirling's approximation for the factorial function, we get the asymptotic reduction factor of $\sqrt{\pi n}$, that is, the relative benefit of using the $\langle\hat{S}_Z\rangle$ conservation filter actually grows with the size of the spin system (Fig. 2). To make this procedure a little less abstract, consider a radical pair (electrons A and B) with a single spin-1/2 nucleus (N). To construct the reduced state list according to the criteria just outlined, we examine

TABLE I. Three noninteracting subspaces of the reduced state space in a simple (and therefore human readable) case of a radical pair (electrons A and B, nucleus N) with a single spin-1/2 nucleus at electron A. The irreducible spherical tensor notation has been converted to product operator notation for clarity. The full state space dimension is 64.

| $p_{\mathrm{A}}=p_{\mathrm{B}}=0$ | $p_{\mathrm{A}}=-p_{\mathrm{B}}=+1$ | $p_{\mathrm{A}}=-p_{\mathrm{B}}=-1$ |
|---|---|---|
| $\hat{E}^{(\mathrm{A})}\otimes\hat{S}_Z^{(\mathrm{B})}\otimes\hat{S}_Z^{(\mathrm{N})}$ | $\hat{E}^{(\mathrm{A})}\otimes\hat{S}_-^{(\mathrm{B})}\otimes\hat{S}_+^{(\mathrm{N})}$ | $\hat{E}^{(\mathrm{A})}\otimes\hat{S}_+^{(\mathrm{B})}\otimes\hat{S}_-^{(\mathrm{N})}$ |
| $\hat{S}_+^{(\mathrm{A})}\otimes\hat{S}_Z^{(\mathrm{B})}\otimes\hat{S}_-^{(\mathrm{N})}$ | $\hat{S}_+^{(\mathrm{A})}\otimes\hat{S}_-^{(\mathrm{B})}\otimes\hat{E}^{(\mathrm{N})}$ | $\hat{S}_-^{(\mathrm{A})}\otimes\hat{S}_+^{(\mathrm{B})}\otimes\hat{E}^{(\mathrm{N})}$ |
| $\hat{S}_Z^{(\mathrm{A})}\otimes\hat{S}_Z^{(\mathrm{B})}\otimes\hat{E}^{(\mathrm{N})}$ | $\hat{S}_+^{(\mathrm{A})}\otimes\hat{S}_-^{(\mathrm{B})}\otimes\hat{S}_Z^{(\mathrm{N})}$ | $\hat{S}_-^{(\mathrm{A})}\otimes\hat{S}_+^{(\mathrm{B})}\otimes\hat{S}_Z^{(\mathrm{N})}$ |
| $\hat{S}_Z^{(\mathrm{A})}\otimes\hat{S}_Z^{(\mathrm{B})}\otimes\hat{S}_Z^{(\mathrm{N})}$ | $\hat{S}_Z^{(\mathrm{A})}\otimes\hat{S}_-^{(\mathrm{B})}\otimes\hat{S}_+^{(\mathrm{N})}$ | $\hat{S}_Z^{(\mathrm{A})}\otimes\hat{S}_+^{(\mathrm{B})}\otimes\hat{S}_-^{(\mathrm{N})}$ |
| $\hat{S}_-^{(\mathrm{A})}\otimes\hat{S}_Z^{(\mathrm{B})}\otimes\hat{S}_+^{(\mathrm{N})}$ | | |

TABLE II. Two out of three (the third subspace is a copy of $p_A=-p_B=+1$ with the signs flipped for all the $m$ quantum numbers in $\hat{T}_{l,m}$) noninteracting subspaces of the reduced state space in a simple (and therefore human readable) case of a radical pair (electrons A and B, nuclei 1 and 2) with two equivalent spin-1/2 nuclei at electron A, written in irreducible spherical tensor notation. The full state space dimension is 256.

| States in $p_A=p_B=0$ | States in $p_A=-p_B=+1$ |
|---|---|
| $\hat{T}^{(A)}_{0,0}\otimes\hat{T}^{(B)}_{1,0}\otimes(\hat{T}^{(1)}_{0,0}\otimes\hat{T}^{(2)}_{1,0}+\hat{T}^{(1)}_{1,0}\otimes\hat{T}^{(2)}_{0,0})$ | $\hat{T}^{(A)}_{0,0}\otimes\hat{T}^{(B)}_{1,-1}\otimes(\hat{T}^{(1)}_{0,0}\otimes\hat{T}_{1,1}+\hat{T}^{(1)}_{1,1}\otimes\hat{T}^{(2)}_{0,0})$ |
| $\hat{T}^{(A)}_{0,0}\otimes\hat{T}^{(B)}_{1,0}\otimes(\hat{T}^{(1)}_{1,1}\otimes\hat{T}^{(2)}_{1,-1}+\hat{T}^{(1)}_{1,-1}\otimes\hat{T}^{(2)}_{1,1})$ | $\hat{T}^{(A)}_{0,0}\otimes\hat{T}^{(B)}_{1,-1}\otimes(\hat{T}^{(1)}_{1,1}\otimes\hat{T}^{(2)}_{1,0}+\hat{T}^{(1)}_{1,0}\otimes\hat{T}^{(2)}_{1,1})$ |
| $\hat{T}^{(A)}_{0,0}\otimes\hat{T}^{(B)}_{1,0}\otimes\hat{T}^{(1)}_{1,0}\otimes\hat{T}^{(2)}_{1,0}$ | $\hat{T}^{(A)}_{1,1}\otimes\hat{T}^{(B)}_{1,-1}\otimes\hat{T}^{(1)}_{0,0}\otimes\hat{T}^{(2)}_{0,0}$ |
| $\hat{T}^{(A)}_{1,1}\otimes\hat{T}^{(B)}_{1,0}\otimes(\hat{T}^{(1)}_{0,0}\otimes\hat{T}^{(2)}_{1,-1}+\hat{T}^{(1)}_{1,-1}\otimes\hat{T}^{(2)}_{0,0})$ | $\hat{T}^{(A)}_{1,1}\otimes\hat{T}^{(B)}_{1,-1}\otimes(\hat{T}^{(1)}_{0,0}\otimes\hat{T}^{(2)}_{1,0}+\hat{T}^{(1)}_{1,0}\otimes\hat{T}^{(2)}_{0,0})$ |
| $\hat{T}^{(A)}_{1,1}\otimes\hat{T}^{(B)}_{1,0}\otimes(\hat{T}^{(1)}_{1,0}\otimes\hat{T}^{(2)}_{1,-1}+\hat{T}^{(1)}_{1,-1}\otimes\hat{T}^{(2)}_{1,0})$ | $\hat{T}^{(A)}_{1,1}\otimes\hat{T}^{(B)}_{1,-1}\otimes(\hat{T}^{(1)}_{1,1}\otimes\hat{T}^{(2)}_{1,-1}+\hat{T}^{(1)}_{1,-1}\otimes\hat{T}^{(2)}_{1,1})$ |
| $\hat{T}^{(A)}_{1,0}\otimes\hat{T}^{(B)}_{1,0}\otimes\hat{T}^{(1)}_{0,0}\otimes\hat{T}^{(2)}_{0,0}$ | $\hat{T}^{(A)}_{1,1}\otimes\hat{T}^{(B)}_{1,-1}\otimes\hat{T}^{(1)}_{1,0}\otimes\hat{T}^{(2)}_{1,0}$ |
| $\hat{T}^{(A)}_{1,0}\otimes\hat{T}^{(B)}_{1,0}\otimes(\hat{T}^{(1)}_{0,0}\otimes\hat{T}^{(2)}_{1,0}+\hat{T}^{(1)}_{1,0}\otimes\hat{T}^{(2)}_{0,0})$ | $\hat{T}^{(A)}_{1,0}\otimes\hat{T}^{(B)}_{1,-1}\otimes(\hat{T}^{(1)}_{0,0}\otimes\hat{T}^{(2)}_{1,1}+\hat{T}^{(1)}_{1,1}\otimes\hat{T}^{(2)}_{0,0})$ |
| $\hat{T}^{(A)}_{1,0}\otimes\hat{T}^{(B)}_{1,0}\otimes(\hat{T}^{(1)}_{1,1}\otimes\hat{T}^{(2)}_{1,-1}+\hat{T}^{(1)}_{1,-1}\otimes\hat{T}^{(2)}_{1,1})$ | $\hat{T}^{(A)}_{1,0}\otimes\hat{T}^{(B)}_{1,-1}\otimes(\hat{T}^{(1)}_{1,1}\otimes\hat{T}^{(2)}_{1,0}+\hat{T}^{(1)}_{1,0}\otimes\hat{T}^{(2)}_{1,1})$ |
| $\hat{T}^{(A)}_{1,0}\otimes\hat{T}^{(B)}_{1,0}\otimes\hat{T}^{(1)}_{1,0}\otimes\hat{T}^{(2)}_{1,0}$ | $\hat{T}^{(A)}_{1,-1}\otimes\hat{T}^{(B)}_{1,-1}\otimes\hat{T}^{(1)}_{1,1}\otimes\hat{T}^{(2)}_{1,1}$ |
| $\hat{T}^{(A)}_{1,-1}\otimes\hat{T}^{(B)}_{1,0}\otimes(\hat{T}^{(1)}_{0,0}\otimes\hat{T}^{(2)}_{1,1}+\hat{T}^{(1)}_{1,1}\otimes\hat{T}^{(2)}_{0,0})$ | |
| $\hat{T}^{(A)}_{1,-1}\otimes\hat{T}^{(B)}_{1,0}\otimes(\hat{T}^{(1)}_{1,1}\otimes\hat{T}^{(2)}_{1,0}+\hat{T}^{(1)}_{1,0}\otimes\hat{T}^{(2)}_{1,1})$ | |

each of the states $\hat{T}^{(A)}_{l_A m_A}\otimes\hat{T}^{(B)}_{l_B m_B}\otimes\hat{T}^{(N)}_{l_N m_N}$ with $(l,m)=\{(0,0),(1,1),(1,0),(1,-1)\}$ for its coherence order $p=m_A+m_B+m_N$, keeping only those with $p=0$. This leaves 20 basis states out of 64.

### C. Noninteracting subspace separation

It is also the case when the two radicals do not interact that the coherence order for each radical is conserved independently, providing a second conservation law filter. The second, third, and fourth terms in both Eq. (27) have $p_A=p_B=0$, $p_A=-p_B=+1$, and $p_A=-p_B=-1$, respectively. Each of these evolves separately as an independent subspace, and this fact is picked up by the subspace analysis procedure described in Sec. II C.

The state in which the operator for every spin is $\hat{T}_{0,0}$ commutes with every other state, and so contributes a constant value to the ultimate product yield (1/4 for an initial singlet and 3/4 for an initial triplet). Similarly, any state in which the operator for every spin in *one* of the radicals is $\hat{T}_{0,0}$ can never be reached and may be discarded. Finally, the third and fourth terms in Eq. (27) are symmetry related and contribute equally to the product yield, thus only one needs to be calculated explicitly. In summary

$$\Phi_S=\tfrac{1}{4}+\Phi_S(p_A=p_B=0)+\Phi_S(p_A=-p_B=+1)+\Phi_S(p_A=-p_B=-1),$$
$$\Phi_S(p_A=-p_B=+1)=\Phi_S(p_A=-p_B=-1). \tag{30}$$

In the case of the single-nucleus radical pair introduced above, we calculate the coherence order of each radical ($p_A=m_A+m_N$, $p_B=m_B$) in the 20 retained states, assigning them to either the $p_A=p_B=0$ subspace or the $p_A=-p_B=+1$ subspace; all other states are discarded. The resulting lists have, respectively, five and four entries (shown in product operator notation in Table I), down from the original 64. A state-by-state run through the pruning procedure is given in the supplementary information.[35]

### D. Basis symmetrization

Because all characters of the $A_{1g}$ irrep are unity, the SALC procedure given by Eq. (12) amounts to basis set symmetrization. We consider now a radical pair with two equivalent spin-1/2 nuclei. After applying the conservation law

TABLE III. Examples of the reductions in the Liouville state space for radical pairs containing different numbers of equivalent spin-1/2 nuclei.

| | | | $p_A=p_B=0$ | | $p_A=-p_B=+1$ | |
|---|---|---|---|---|---|---|
| Symmetry of nuclei in radical A | Symmetry of nuclei in radical B | Total state space | Subspace size | Percentage of total state space | Subspace size | Percentage of total state space |
| $C_2$ | – | 256 | 11 | 4.3 | 9 | 3.5 |
| $C_3$ | – | 1024 | 19 | 1.9 | 16 | 1.6 |
| $C_3$ | $C_2$ | 16 384 | 209 | 1.3 | 144 | 0.88 |
| $C_3,C_3$ | – | 65 536 | 291 | 0.44 | 262 | 0.40 |
| $C_4$ | $C_3$ | 262 144 | 551 | 0.21 | 400 | 0.17 |
| $C_2,C_2,C_2,C_2$ | – | 1 048 576 | 6843 | 0.65 | 6254 | 0.60 |
| $C_6$ | $C_2$ | 1 048 576 | 605 | 0.058 | 441 | 0.042 |
| $C_8$ | – | 1 048 576 | 89 | 0.0085 | 81 | 0.0077 |

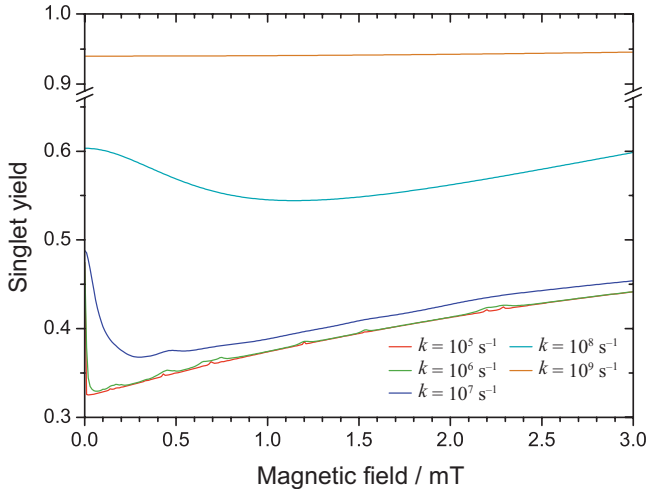


FIG. 3. Simulated magnetic field effects on the singlet product yield of a radical pair comprising benzyl and a radical with no hyperfine couplings, calculated in the reduced Liouville space. Values of the rate constant $k$ are as shown. Spin relaxation is not included. The two radicals were assumed to have identical $g$-values (2.0023). Hyperfine coupling constants are shown in millitesla (mT) in Scheme 1.

pruning and subspace separation as described above, the state space dimension is reduced from 256 to $19 \oplus 15$. Symmetrization using Eq. (14) reduces this to $11 \oplus 9$ (Table II).

### E. Superoperator construction

The states in the restricted basis may be examined sequentially and Eqs. (20), (24), and (25) used to form the reduced Liouvillian, with care taken to account for every term in the symmetrized states. The singlet yield may then be calculated using Eq. (29) for each of the components of the initial state in Eq. (27). Table III shows the resulting reduction in the state space dimension for several types of radical pairs. Symmetry is a frequently occurring property in EPR systems, and if there are, e.g., six equivalent nuclei in one radical and two in the other, the two state spaces are 605 ($p_A = p_B = 0$) and 441 ($p_A = -p_B = +1$), i.e., 0.058% and 0.042%, respectively, of the full $4^{10} = 1\,048\,576$ dimensional state space. Given the cubic scaling of many matrix operations, this is clearly a very significant reduction. It is even more remarkable that this reduction is exact.

### F. Simulation results

To demonstrate the scope of these procedures, we simulate the effects of applied magnetic fields on the reactions of three model radical pairs. In all three cases, the initial state was singlet. Figure 3 shows the yield of the singlet product formed from the recombination of the benzyl radical[36] and a radical with negligible hyperfine interactions, calculated using Eq. (29) with $\hat{\hat{R}} = 0$. Isotropic hyperfine couplings were taken from the work of Dust and Arnold[37] [Scheme 1(a)]. The reduced state spaces have dimensions of 2933 and 2646, some 90 times smaller than the full Liouville space of $4^9 = 262\,144$. The dependence on the magnetic field strength and the recombination rate constant is qualitatively as expected[32] and identical to the results of Hilbert-space calculations (not shown). The pronounced drop in $\Phi_S$ observable for the longer lived radical pairs in weak fields is known as the "low field effect."[32,34]

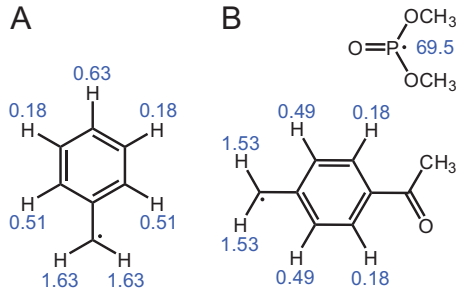


SCHEME 1.

The principal motivation for wishing to perform simulations such as these in Liouville space, rather than the much smaller Hilbert space, is the need to include incoherent processes such as spin relaxation. Figure 4 shows results for a radical pair comprising dimethoxyphosphonyl and *p*-acetylbenzyl, simulated using reduced lists of just 3875 and 2764 states (the full state space is again 262 144). Isotropic hyperfine coupling data were taken from the work of Dust and Arnold[37] [Scheme 1(b)], ignoring nuclei with couplings less than 0.1 mT. The phosphorus in dimethoxyphosphonyl has a much larger anisotropic hyperfine interaction than any other nuclear spin and is assumed to dominate the spin relaxation that results from rotational motion in solution. All other hyperfine anisotropies were neglected. A template relaxation matrix for the interacting phosphorus-electron pair was determined using Bloch–Redfield–Wangness relaxation theory, by means of a symbolic processing procedure,[38] in the extreme narrowing limit, i.e., $\omega^2 \tau_c^2 \ll 1$ ($\tau_c$ is the isotropic rotational correlation time of the radical and $\omega$ is the largest energy-level difference in the spin system). The resulting superoperator was then projected into the reduced state space by noting that the other spins are unaffected by this relaxation process. Magnetic field effects were simulated for a range of values of the self-relaxation rate, $\chi = \frac{1}{6}(\Delta A^2 + 3\delta A^2)\tau_c = [A:A]\tau_c$, where $\Delta A$ is the axiality and $\delta A$ the rhombicity of the phosphorus hyperfine tensor. Literature values of $\tau_c$ (2.4 ps) and $[A:A]$ (186 mT$^2$) were used.[39] As expected, an increase in the relaxation rate causes the singlet product yield $\Phi_S$ to approach the statistical value of 0.25. Faster relaxation also attenuates the low field effect and smoothes out the "wrinkles" that arise from avoided crossings of energy levels.[40]

A final example (Fig. 5) illustrates the application of state space restriction to radicals containing nuclei with spin quantum numbers $I > 1/2$. There have been reports that the kinetics of enzymatic synthesis of adenosine triphosphate (ATP) from adenosine diphosphate (ADP) exhibit a magnesium isotope effect (IE) and are sensitive to applied magnetic fields.[41,42] Both effects, it has been suggested, could arise from a radical pair intermediate, [$Mg^{\bullet+}ADP^{\bullet-}$] with isotope-dependent magnetic properties ($^{25}$Mg has spin-5/2, while $^{24}$Mg and $^{26}$Mg are nonmagnetic). Although there appears to be scant independent support for a free radical mechanism, the proposed reaction (Fig. 6) provides a convenient example

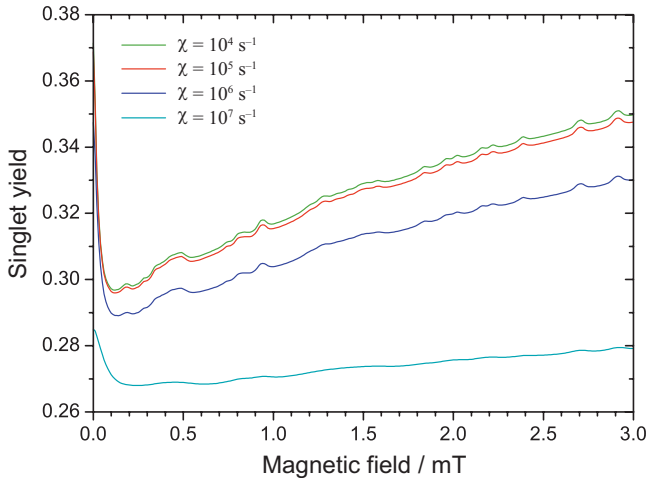


FIG. 4. Simulated magnetic field effects on the singlet product yield of a dimethoxyphosphonyl-*p*-acetylbenzyl radical pair. Values of the relaxation rate $\chi$ are as shown. The recombination rate constant, $k=10^6$ s$^{-1}$. The two radicals were assumed to have identical *g*-values (2.0023). Hyperfine coupling constants are shown in mT in Scheme 1.

of the use of state space restriction. Simulation of this reaction scheme requires a kinetic superoperator, $\hat{\hat{K}}$, as in Eq. (9), rather than the simple exponential model used above:[43]

$$\hat{\hat{K}} = -\tfrac{1}{2}k_{-1}(\hat{Q}_S \otimes \hat{E} + \hat{E} \otimes \hat{Q}_S^T) - k_P\hat{\hat{E}}. \tag{31}$$

The $k_{-1}$ term represents the spin-selective back reaction of the singlet radical pair while the $k_P$ term is the spin-independent forward reaction. The singlet projection superoperator, $\hat{Q}_S$, couples the two radicals which means that the individual radical coherence orders are not conserved. Separation of $\hat{\rho}(0)$ into its component operators, Eq. (30), therefore does not reduce the state space in this case as the subspaces no longer evolve independently. The IE on the steady state rate of product formation was calculated as[43]

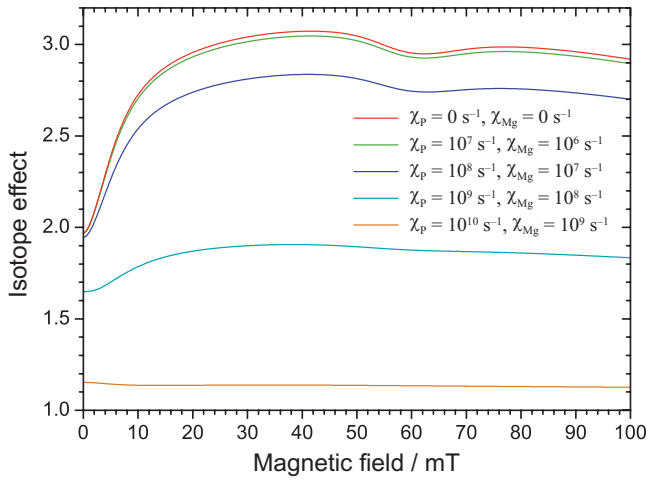


FIG. 5. Simulated magnetic field effects on the Mg IE of the reaction shown in Fig. 6. Values of the relaxation parameters $\chi_P$ and $\chi_{Mg}$ are as shown. Rate constants: $k_{-1}=10^{10}$ s$^{-1}$ and $k_P=10^8$ s$^{-1}$. Isotropic hyperfine interactions: $a_P=3$ mT and $a_{Mg}=21$ mT. The IE is defined in Eq. (32). Given the large hyperfine coupling constant of $Mg^{\bullet+}$, the extreme narrowing limit is not strictly valid, so that the simulations are likely to overestimate relaxation effects. The two radicals were assumed to have identical *g*-values (2.0023).

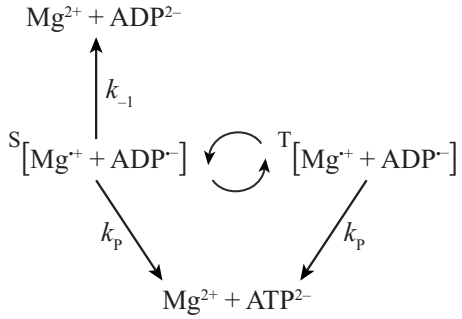


FIG. 6. Reaction scheme (Ref. 41) used as an illustration of restricted Liouville space spin dynamics simulation including a kinetics and relaxation superoperators.

$$\mathrm{IE}(B) = \frac{\mathrm{Tr}[^{25}\hat{\hat{L}}(B)^{-1}\hat{Q}_S]}{\mathrm{Tr}[^{24,26}\hat{\hat{L}}(B)^{-1}\hat{Q}_S]} \tag{32}$$

for a magnetic field $B$, where the superscript refers to the magnesium isotope. The rotational correlation time of the enzyme-ATP complex has been estimated at $\tau_c \approx 30$ ns.[44] A simple estimate shows that the terminal phosphorus nucleus in $ADP^{\bullet-}$ is expected to induce relaxation at least ten times faster than the magnesium due to its larger hyperfine anisotropy, and with this factor in mind a range of $\chi$ values was chosen for simulation, Fig. 5. The isotropic hyperfine couplings were taken from Ref. 43 This calculation has a full state space of 64 and 2304 for $[^{24,26}Mg^{\bullet+}\ ADP^{\bullet-}]$ and $[^{25}Mg^{\bullet+}\ ADP^{\bullet-}]$, respectively, which are reduced to 20 and 324 by our techniques. As expected, when the relaxation ($\chi_P$ and/or $\chi_{Mg}$) becomes faster than the smaller of the two rate constants (i.e., $k_P$, see figure caption), the effect is to attenuate the calculated magnetic IE.

## V. CONCLUSIONS

The theoretical arguments and numerical simulations presented above suggest that, contrary to intuitive expectations, the state space restriction approach[1–3] can be very efficient even in small and densely coupled spin systems. The algebraic properties of active spaces explored in this paper provide state space truncation criteria that are relevant and directly applicable to most practically encountered EPR and spin chemistry cases. In all systems the authors worked with so far at least one of the methods (including those reported in our earlier papers)[1,2] is applicable and yields very significant reduction in state space dimension. Essentially, the conclusion that we had initially reached for NMR stands in these systems as well—the state space dimension actually required for EPR and spin chemistry simulations is orders of magnitude smaller than the full state space dimension, and polynomially scaling algorithms exist for many practically encountered spin systems.

## ACKNOWLEDGMENTS

This work was supported by EPSRC (Grant Nos. EP/F065205/1 and EP/H003789/1) and NIS (Grant No. PHY05-51164). The authors are grateful to Chris Rodgers, Matthew Krzystyniak, Gareth Charnock, and Alice Bowen for stimu-

lating discussions. I.K. gratefully acknowledges the Kavli Institute for Theoretical Physics at UCSB.

[1] I. Kuprov, N. Wagner-Rundell, and P. J. Hore, J. Magn. Reson. **189**, 241 (2007).
[2] I. Kuprov, J. Magn. Reson. **195**, 45 (2008).
[3] M. C. Butler, J. N. Dumez, and L. Emsley, Chem. Phys. Lett. **477**, 377 (2009).
[4] G. Moro and J. H. Freed, J. Chem. Phys. **74**, 3757 (1981).
[5] K. V. Vasavada, D. J. Schneider, and J. H. Freed, J. Chem. Phys. **86**, 647 (1987).
[6] N. C. Nielsen, T. Schulteherbruggen, and O. W. Sorensen, Mol. Phys. **85**, 1205 (1995).
[7] A. Wokaun and R. R. Ernst, Mol. Phys. **36**, 317 (1978).
[8] P. L. Corio, *Structure of High-Resolution NMR Spectra* (Academic, New York, 1966).
[9] H. Weyl, *The Theory of Groups and Quantum Mechanics* (Dover, New York, 1931).
[10] E. P. Wigner, *Group Theory and its Application to the Quantum Mechanics of Atomic Spectra* (Academic, New York, 1964).
[11] J. Kowalewski, D. Kruk, and G. Parigi, Adv. Inorg. Chem. **57**, 41 (2005).
[12] J. Kowalewski, C. Luchinat, T. Nilsson, and G. Parigi, J. Phys. Chem. A **106**, 7376 (2002).
[13] A. A. Nevzorov and J. H. Freed, J. Chem. Phys. **112**, 1425 (2000).
[14] E. Meirovitch and J. H. Freed, J. Phys. Chem. **84**, 2459 (1980).
[15] A. G. Redfield, IBM J. Res. Dev. **1**, 19 (1957).
[16] M. Goldman, J. Magn. Reson. **149**, 160 (2001).
[17] G. James and M. Liebeck, *Representations and Characters of Groups*, 2nd ed. (Cambridge University Press, Cambridge, 2001).
[18] J. A. Weil and D. F. Howarth, J. Magn. Reson. **197**, 28 (2009).
[19] D. M. Brink and G. R. Satchler, *Angular Momentum* (Clarendon, Oxford, 1993).
[20] N. L. Biggs, *Algebraic Graph Theory* (Cambridge University Press, London, 1974).
[21] H. N. Gabow and R. E. Tarjan, J. Comput. Syst. Sci. **30**, 209 (1985).
[22] R. Tarjan, SIAM J. Comput. **1**, 146 (1972).
[23] J. L. Gross and J. Yellen, *Graph Theory and its Applications*, 2nd ed. (Chapman & Hall, London, 2006).
[24] R. R. Ernst, G. Bodenhausen, and A. Wokaun, *Principles of Nuclear Magnetic Resonance in One and Two Dimensions* (Clarendon, Oxford, 1987).
[25] M. Mehring and V. A. Weberruss, *Object-Oriented Magnetic Resonance: Classes and Objects, Calculations and Computations* (Academic, San Diego, Calif.; London, 2001).
[26] I. Kuprov, N. Wagner-Rundell, and P. J. Hore, J. Magn. Reson. **190**, 76 (2007).
[27] R. Brüschweiler and R. R. Ernst, J. Magn. Reson. **124**, 122 (1997).
[28] U. E. Steiner and T. Ulrich, Chem. Rev. (Washington, D.C.) **89**, 51 (1989).
[29] C. T. Rodgers, Pure Appl. Chem. **81**, 19 (2009).
[30] L. T. Muus, *Chemically Induced Magnetic Polarization* (Reidel, Dordrecht, Holland, 1977).
[31] B. Brocklehurst, Chem. Soc. Rev. **31**, 301 (2002).
[32] C. R. Timmel, U. Till, B. Brocklehurst, K. A. McLauchlan, and P. J. Hore, Mol. Phys. **95**, 71 (1998).
[33] R. Kaptein and J. L. Oosterhoff, Chem. Phys. Lett. **4**, 195 (1969).
[34] B. Brocklehurst, J. Chem. Soc., Faraday Trans. 2 **72**, 1869 (1976).
[35] See supplementary material at http://dx.doi.org/10.1063/1.3398146 for the full details of the pruning procedure.
[36] N. V. Lebedeva, M. V. Fedin, E. G. Bagryanskaya, and R. Z. Sagdeev, Phys. Chem. Chem. Phys. **5**, 2595 (2003).
[37] J. M. Dust and D. R. Arnold, J. Am. Chem. Soc. **105**, 1221 (1983).
[38] I. Kuprov, N. Wagner-Rundell, and P. J. Hore, J. Magn. Reson. **184**, 196 (2007).
[39] M. V. Fedin, H. Yashiro, P. A. Purtov, E. G. Bagryanskaya, and M. D. E. Forbes, Mol. Phys. **100**, 1171 (2002).
[40] E. V. Kalneus, A. A. Kipriyanov, P. A. Purtov, D. V. Stass, and Y. N. Molin, Dokl. Phys. Chem. **415**, 170 (2007).
[41] A. L. Buchachenko, D. A. Kouznetsov, M. A. Orlova, and A. A. Markarian, Proc. Natl. Acad. Sci. U.S.A. **102**, 10793 (2005).
[42] A. L. Buchachenko and D. A. Kuznetsov, J. Am. Chem. Soc. **130**, 12868 (2008).
[43] A. L. Buchachenko, N. N. Lukzen, and J. B. Pedersen, Chem. Phys. Lett. **434**, 139 (2007).
[44] D. Hornikova, P. Herman, J. Mejsnar, J. Vecer, and J. Zurmanova, Biochim. Biophys. Acta **1794**, 270 (2009).